RSC Advances

ROYAL SOCIETY OF CHEMISTRY

www.rsc.org/advances

The Magnetic and Optical Properties of 3d transition metal doped SnO_2 Nanosheets

Yong Feng, Wei-Xiao Ji, Bao-Jun Huang, Xin-lian Chen, Feng Li, Ping Li,
Chang-wen Zhang, Pei-Ji Wang *
School of Physics, University of Jinan, Jinan 250022, People's Republic of China

Abstract :

Based on first-principles calculations, we study on the electronic structure, magnetic properties and optical properties of the TM atom doped SnO_2NSs. Computational results indicate that the pristine SnO_2NSs is a direct gap semiconductor with nonmagnetic states. The Cr, Mn, Fe atom doping can induce 2 μ_B, -3 μ_B and 2 μ_B magnetic moment respectively, while the Ni atom doped SnO_2NSs keeps the nonmagnetic states. More interestingly, the Fe doped SnO_2NSs becomes an indirect gap semiconductor, and the Cr, Mn and Ni atom doping remain the character of direct gap semiconductor. For optical properties, the optical absorption edge shows red shift phenomenon for TM atom (Cr, Mn, Fe or Ni) doped SnO_2NSs. In addition, the tensity of absorption, reflection and refraction coefficient are enhanced significantly in visible light region, which may be very useful to design the solar cells, photoelectronic devices and photocatalysts.

KEYWORDS: SnO_2 nanosheets, electronic structure, magnetic properties, optical properties

1. Introduction

Dilute magnetic semiconductors (DMSs) have attracted extensive attentions in experimental and theoretical because of their potential application in spintronic devices[1-5]. For practical applications, it is required that DMSs are half-metallic (HM) or ferromagnetic (FM) around room temperatures. However, DMSs usually have rather low Curie temperature (T_C), so it is desirable find a new method to improve T_C of DMSs. Recently, the reported DMSs can obtain high T_C by doping transition metal (TM) elements, such as ZnO[6-8], In_2O_3[9], TiO_2[10], CeO_2[11] and so on.

As a typical wide-gap semiconductor with band gap E_g=3.6eV, SnO_2 has received considerable interest for its wide variety of practical applications, such as photovoltaic devices, transparent conducting electrodes, gas sensors, solar cells, panel displays and ferroelectric transparent thin-film transistors[12-17]. More recently, TM-doped SnO_2 become one of the hottest research topics in spintronics. Room temperature (RT) ferromagnetism has been observed in V[18], Cr[19,20], Mn[21], Fe[22,23], Co[24] and Ni[25] doped SnO_2. By now these researches mainly concentrate on SnO_2 bulk while seldom report about SnO_2 nanosheets from the theoretical calculations. The nanosheets structure may have many excellent properties because of its' larger specific surface area. SnO_2 nanosheets have higher lithium storage properties with high reversible capacities and good cycling performance due to large specific surface area. [26] Compared to SnO_2 bulk, SnO_2NSs with larger band gap are more suitable for tuning band gap to obtain better optical properties. And high optical transmittance[27], well gas-sensing optical properties are

*Corresponding author: School of Physics, University of Jinan, Jinan 250022, China
Tel: +86 531 82765965. E-mail adress: ss_wangpj@ujn.edu.cn （Pei-ji Wang）

found in transition metal doped SnO_2 film. More interestingly, SnO_2 nanosheets (NSs) was by fabricated Wang *et al*.[28] in experiments, and its T_C was estimated to be about 300 ºC, indicated its potential value in spintronic devices. The results provide an opportunity to study the two-dimensional (2D) SnO_2NSs. Gul Rahman *et al*.[29] reported intrinsic magnetism in nanosheets of SnO_2 and it is easier to create vacancies，which are magnetic, at the surface of the sheets for SnO_2NSs different thicknesses. Research by Luan *et al*.[30], they find a strong localized magnetic moment in Co-doped SnO_2NSs. For optical properties, Huang[31] reported the absorb capacity become stronger in visible region with increasing Ag concentrations doped SnO_2NSs.

In the present work, we perform first principles calculations to study on the electronic, magnetic and optical properties of TM element doped SnO_2NSs, where TM atom substitute Sn atom for Cr, Mn, Fe or Ni in 2D SnO_2NSs. Our results show the doped TM atom could induce magnetic moment, except Ni, and the magnetic moment mainly comes from 3d orbital of TM atom. The optical properties can get significantly improved in visible region.

2. Computational details

The electronic properties and band structures are performed employing the vienna ab initio simulation package (VASP)[32], and the optical properties are carried out by using the WIEN2k simulation package which implements full potential linearized augmented plane wave (FLAPW) method[33]. The exchange-correlation (XC) functional is approximated with the generalized gradient approximation (GGA)[34] and GGA+U[35] as proposed by the Perdew-Bueke-Emzerhof (PBE). And a 400 eV cutoff energy for the plane-wave basis set are used. Two-dimensional periodic boundary conditions are applied to the TM-doped SnO_2NSs while a vacuum region of 12 Å is set along the direction perpendicular to the SnO_2NSs surface to avoid the mirror interaction. The k-point meshes for Brillouin zone are generated using a 9×9×1 Monkhorst-Pack grid[36]. All atomic positions in all structures are fully relaxed until all atomic forces have converged to be less than 0.02 eV/Å.

3. Results and discussion

3.1 Formation energy：

Firstly, we carry out the pristine SnO_2NSs which is modeled with a 4×4×1 supercell containing sixteen SnO_2 units, as shown in Fig. 1. We can find that it forms a sandwiched structure from the side view of SnO_2NSs Fig.1(b). These structures are similar to MoS_2NSs[37] and TiO_2NSs[38] in previous report. In the top view of SnO_2NSs Fig. 1(a), the tin atom is substituted by TM atom at the site of *X*. The optimized lattice parameters are 3.2 Å and the length of Sn-O bond is 2.11 Å, which consistent with the Luan's[30] research. In Fig.1(c), we show the total density of states (TDOSs) for pristine SnO_2NSs. It presents a nonmagnetic behavior due to the electron wave function dose not exhibit spin polarization in spin-up and spin-down channels. The band structure of pristine SnO_2NSs as shown in Fig.1(d). The band gap is about 2.75eV, which is more nearly experimental value compared with Huang's[31] report. Thus the pristine SnO_2NSs is also a direct gap semiconductor, which is agreement with the bulk SnO_2 calculated results[39-40].

Next, we perform the effect of TM atom (Cr, Mn, Fe or Ni) substitution for Sn atom in SnO_2NS. The doping atom is located *X* sit in Fig.1 (a). In order to evaluate the stability of TM-doped SnO_2NSs, we calculate the defect formation energy (E_f) defined as $E_f = E_{X:SnO_2} - E_{SnO_2} + u_{Sn} - u_x$ [41], where $E_{X:SnO_2}$ and E_{SnO_2} are the total energies of the TM-doped SnO_2NSs and SnO_2NSs supercell, and u_{Sn}, u_x are the chemical potentials of Sn and TM atom(Cr, Fe, Mn or Ni), respectively. The values of E_f are shown in Table I. Compared with pristine SnO_2NSs, the Cr, Mn doped SnO_2NSs release 0.56eV, 0.37eV in energy and Fe, Ni doped SnO_2NSs absorb 0.35eV, 1.75eV in energy, respectively. This indicates that Cr, Mn as a dopant can obtain a more stable structure than pristine SnO_2NSs. After structural optimization, we find all the bond length of TM-O bond (d_{x-o}) less than Sn-O bond (2.11 Å) in Table I because of smaller ionic radius of TM atom (Cr, Fe, Mn or Ni) substitute Sn atom. And the bond length of TM-O atom gets shorter with the increase of atomic number.

3.2 Electronic structures and magnetic properties

The TDOSs and partial density of states (PDOSs) for TM atom (Cr, Fe, Mn or Ni) doped SnO_2NSs are illustrated in Fig. 2 (a)-(d), respectively. Taking the Cr-doped SnO_2NSs as a representative example from Fig. 2(a), the electronic states of valence band mainly arise from the strong hybridization between O 2p and Sn 5p states, while Sn 5s states make mainly contribution to the electronic states of conduction band. We also observe that the Fermi level shifts upward to the conduction band, indicating n-type conductivity character, which may display the low resistivity character. Moreover, there exist some impurity energy levels near fermi level which are mainly supplied by Cr 3d, O 2p and Sn 5p states. The Fe-, Mn-, Ni-doped SnO_2NSs can obtain the similar conclusion by analyzing the DOS. However, compared with other three TM atom (Cr, Fe, Mn) doped SnO_2NSs, the difference of Ni-doped SnO_2NSs is that symmetrical distribution of the wave functions of spin-up and spin-down channels on TDOSs. The result indicates that the others doped structures with magnetic except Ni-doped SnO_2NSs. DOS analysis further shows that the magnetic moment is mainly from TM atom 3d orbital.

In order to study the origin of magnetic, we perform the spin-polarized calculation and the spin density distributions are displayed in Fig. 3. We can find a strong localized magnetic moment except Ni-doped SnO_2NSs and the magnetic mainly origins from the doped atom. The Cr, Fe atom supplies the spin-up magnetic moment and Mn atom provides the spin-down magnetic moment, while Ni atom doesn't provide the magnetic moment. To further verify the localization of the magnetic moment, we calculate the net magnetization defined as $m(r) = \rho_{\uparrow}(r) - \rho_{\downarrow}(r)$, where $\rho_{\uparrow}(r)$ $\rho_{\downarrow}(r)$ is the charge density in spin-up and spin-down channel. The corresponding values of magnetic moment are shown in Table I. The total magnetic moment (*M*) of Cr, Mn, Fe and Ni doped SnO_2NSs are found to be $2\,\mu_B$, $-3\,\mu_B$, $2\,\mu_B$ and $0\,\mu_B$, which the Cr, Mn, Fe atom provide $1.97\,\mu_B$, $-2.85\,\mu_B$, $1.91\,\mu_B$ local magnetic moment (M_x), respectively. The results are similar to the case of TM atom doped TiO_2 carried out by Erricio *et al*[42]. Each doped TM atom contributes two valence electrons to nearest O atom, and the unpaired electrons in Cr, Mn, Fe atom induce the local magnetic moment. The mechanism can be understood as follow: a Cr atom loses two 3d-electrons and one electrons of 4s electron transition to 3d

orbit form a paired electrons, two unpaired electrons provide 1.97 μ_B spin-up local magnetic moment for Cr atom. However, the Mn and Fe atom lose two 3d-electrons forming three unpaired spin-down electrons and two unpaired spin-up electrons, respectively. The magnetic moment can be widely applied to spintronic devices. The charge transfer (Q) for TM atom can be obtained from Bader analysis in Table I. We can find that the number of losing electron Cr, Mn, Fe and Ni atom are 1.80, 1.73 1.57 and 1.34, which the number of electron less than 2 due to the TM atom and O atom form covalent bonds. We also find that the losing electron number tend to drop off with the increase of atomic number. The reason is that the electronegativity of atom is gradually strengthened.

Further, the band structures of TM atom (Cr, Mn, Fe or Ni) doped SnO_2NSs are illustrated in Fig. 4. In Fig. 4, the arrows ↑ and ↓ represent spin-up and spin-down, respectively. Around the Fermi level, there emerge some rather localized energy bands which mainly originate from 3d states of TM atom. The emergence of impurity energy levels may make electronic transition more active from the occupied bands to the unoccupied. This may be helpful to improve the optical properties. For the case of Cr, Mn, and Ni doping, the band structure still remains the character of direct gap semiconductor, while Fe doped SnO_2NSs become an indirect gap semiconductor. We can obtain the same conclusion with DOS from band structures: the Cr, Mn, and Fe doped SnO_2NSs can introduce magnetic moment while Ni atom can not.thes

Unfortunately, GGA method usually underestimates the binding energy of *d* states and yield incorrect behavior for strongly correlated magnetic systems. In order to check our results, we include an on-site Coulomb correlation interaction as given by the GGA+U method, where U (U= 3.0eV) are used to TM atom 3*d* orbit. This is essential for obtaining accurate of band structures and band gaps[43]. The Sn atom 4*d* orbit far from the Fermi level and has little impact on the magnetic properties. In Fig. 5, we show the total DOS and partial DOS with GGA+U method. Comparing with the GGA results, the Fermi energy level shifts down to the valence band, and the amount of impurity energy level is declined around the Fermi energy level. More interestingly, the band gap of GGA+U method is larger than GGA method, which the GGA underestimates the TM atom 3*d* orbitals hybridize quite strongly with oxygen 2p orbitals. The magnetic moments of GGA+U are listed in Table I. We can find that the GGA+U method obtain the same results in magnetic, which indicate that the results of GGA method can qualitatively reflect the properties of TM atom doped SnO_2NS. The band gap slightly increased and magnetic moments invariant demonstrate that the results of GGA method are reliable.

3.3 Optical properties

The optical properties of TM atom doped SnO_2NSs are also calculated in our work. The optical properties of the medium can be derived from the complex dielectric function $\varepsilon(\omega)=\varepsilon_1(\omega)+i\varepsilon_2(\omega)$ [44]. The real part of the dielectric function $\varepsilon_1(\omega)$ can be evaluated from the imaginary part via the Kramers–Kronig transform, and the imaginary part of the dielectric function $\varepsilon_2(\omega)$ momentum matrix elements between the occupied and unoccupied electronic states. The imaginary part of the dielectric function formulas are as following [45].

$$\varepsilon_2(\omega)=\frac{4\pi^2}{m^2\omega^2}\sum_{V,C}\int_{BZ}d^3k\frac{2}{2\pi}\left|e\cdot M_{cv}(K)\right|^2\times\delta[E_C(k)-E_V(k)-\hbar\omega]$$

where subscripts C and V represent conduction band and valence band, respectively, BZ is the first Brillouin zone, k is reciprocal lattice vector, ω is angular frequency, $E_V(k)$ and $E_C(k)$ are intrinsic energy lever of valence band and conduction band, respectively, $|M_{cv}(K)|^2$ is momentum matrix element.

The imaginary part spectrum of dielectric function for pristine and TM atom doped SnO_2NSs are shown in Fig. 6(a). The intensity of $\varepsilon_2(\omega)$ for TM atom doping is stronger than pure SnO_2 nanosheets especial in low energy region. The reason is that some impurity energy levels emerge around Fermi level and the probability of electron transition becomes more common when Sn atom is replaced by TM atom. For Fe doped SnO_2NSs, there are two obvious peaks located at 0.2 eV and 0.6eV. These peaks are mainly ascribed to the transition between Fe 3d states and Sn 5s, 5p states. There is one obvious peak at 0.5eV for Cr doped SnO_2NSs. The reason is analyzed that the band transition from Cr 4s orbital to Cr 3d orbital. There are some other peaks, and the tensity of dielectric function is larger than pure SnO_2NSs in visible light region for all TM doping model, which indicates that the TM doped SnO_2NSs are more suitable for the visible photoelectric devices compared with pure SnO_2NSs. In ultraviolet region, the trend and peaks of TM atom doping are similar to pure SnO_2NSs. As we all know, the absorption property of semiconductor is related to its electronic band structure. The absorption coefficient can be defined as follow: $I(\omega)=\sqrt{2}\omega\left[\sqrt{\varepsilon_1^2(\omega)-\varepsilon_2^2(\omega)}-\varepsilon_1(\omega)\right]^{1/2}$ In Fig. 6(b), we can see that the capacity of absorption is improved in low energy region, which demonstrates that the TM atom doped SnO_2NSs is more suitable to make a photodetector than pure SnO_2NSs. And some peaks emerge in visible light region which are agreed with the imaginary part spectrum of dielectric function. These peaks are ascribed to the interband transition between the TM 3d states and O 2p states. Interestingly, the absorption edges of TM doped SnO_2NSs all show red shift phenomenon, which are caused by the impurity energy levels near Fermi level. The absorption edges of Cr, Fe or Ni doped SnO_2NSs are below 1.50eV which are lower than Mn doped SnO_2NSs whose absorption edge locate at around 2.20eV. The result indicates that Cr, Fe or Ni doped SnO_2NSs have better optical properties compared with Mn doped in visible region. But the all doped models obtain more widely absorption region than pure SnO_2NSs. This results display that the TM doped SnO_2NSs can be widely used in infrared and visible photodetector.

The reflectivity and refractivity of pure SnO_2NSs and TM atom doped SnO_2NSs are calculated in Fig. 7. The reflectivity and refractivity enhance much in low energy region, which also mainly originate from the impurity energy levels near Fermi level. At the Fermi energy level, the value of refraction of pristine and Cr, Mn, Fe, Ni doped SnO_2NSs are 1.181, 1.232, 1.192, 1.247, 1.203, respectively. The Fe doped SnO_2NSs obtain the best effect while there has the minimum influence for Mn doped SnO_2NSs. The same effect of TM doping is suitable for reflectivity. The location of reflectivity and refractivity peaks are also agreed with imaginary part spectrum of dielectric function. In conclusion, the optical properties of TM atom doped SnO_2NSs can get significantly improved in low energy region, while the effect is less obvious in ultraviolet region.

4. Conclusion

In summary, we performed first-principles study on electronic structure, magnetic and optical properties of the TM atom doped SnO_2NSs. Computational results indicate that the pristine SnO_2NSs is a direct gap semiconductor with nonmagnetic states. The Cr, Mn, Fe atom doping can induce the magnetic moment which the value is $2\,\mu_B$, $-3\,\mu_B$ and $2\,\mu_B$, respectively, while the Ni atom doped SnO_2NSs remains the nonmagnetic. The magnetic moment is mainly from TM atom 3d orbital. More interestingly, the Cr, Mn and Ni atom doped SnO_2NSs still remains the character of direct gap semiconductor except Fe atom doping. For optical properties, the the absorption edge shifts to low energy region compared to pure SnO_2NSs. More interestingly, the tensity of absorption, reflection and refraction coefficient are enhanced significantly in visible light region. The results indicate that we fabricate the model about TM atom doped SnO_2NSs may be very useful to design the solar cells, photoelectronic devices and photocatalysts.

Acknowledgements

This work was supported by the National Natural Science Foundation of China (Grant No. 61172028, 11274143 and 11304121), the Natural Science Foundation of Shandong Province (Grant No. ZR2010EL017 and ZR2013AL004), the Research Fund for the Doctoral Program of University of Jinan (Grant No. XBS1433, XBS1402 and XBS1452)

References

[1] Y.W. Son, M.L. Cohen, S.G. Louie, Nature. 444 (2006) 347.
[2] E. Kan, L. Yuan, J.L. Yang, J. Appl. Phys. 102 (2007) 033915.
[3] S. A. Wolf, D. D. Awschalom, R. A. Buhrman, J. M. Daughton, S. von Molnar, M. L. Roukes, A.Y. ChtchelkanVOa and D. M. Treger, Science. 294, (2001) 1488.
[4] S. B. Ogale, R. J. Choudhary, J. P. Buban, S. E. Lo and, S. R. Shinde, S. N. Kale, V. N. Kulkarni, J. Higgins, C. Lanci, J. R. Simpson, N. D. Browning, S. Das Sarma, H. D. Drew, R. L. Greene and T. Venkatesan, Phys. Rev. Lett. (2003) 077205.
[5] T. Fukumura, Z. Jin, A. Ohtomo, H. Koinuma, and M. Kawasaki, Appl. Phys. Lett. 75 (1999) 3366.
[6] Y. Liu, Y. Yang, J. Yang, Q. Guan, H. Liu, L. Yang, Y. Zhang, Y. Wang, M. Wei, X. Liu, L. Fei, X. Cheng, J. Solid State Chem. 184 (2011) 1273.
[7] D.A. Schwartz, K.R. Kittilstved, D.R. Gamelin, Appl. Phys. Lett. 85 (2004) 1395.
[8] J.H. Shim, T. Hwang, S. Lee, J.H. Park, S.J. Han, Y.H. Jeong, Appl. Phys. Lett. 86 (2005) 082503.
[9] N. H. Hong, J. Sakai, N. T. Huong, and V. Brize, Appl. Phys. Lett. 87 (2005) 102505.
[10] N. H. Hong, J. Sakai, and W. Prellier, Phys. Rev. B. 70 (2004) 195204.
[11] Q.Y. Wen, H.W. Zhang, Y.Q. Song, Q.H. Yang, H. Zhu, J.Q. Xiao, J. Phys.: Condens. Matter 19. (2007) 246205.
[12] A. Nuruddin, J. R. Abelson, Thin Solid Films. 394 (2001) 49-63.
[13] Y.S. Zhang, K. Yu, G.D. Li, D.Y. Peng, Q.X. Zhang, H.M. Hu, F. Xu, W. Bai, S.X. Ouyang, Z.Q. Zhu, Appl. Surf. Sci. 253 (2006) 792-796.
[14] S. Ferrere, A. Zaban, B. A. Gsegg, J. Phys. Chem. B. 101 (1997) 4490-4493.
[15] M. Khan, J.N. Xu, N. Chen, W.B. Cao, J. Alloys Compd. 513 (2012) 539-545.
[16] H.C. Wu, Y.C. Peng, C.C. Chen, Opt. Mater. 35 (2013) 509-515.
[17] Z. Y. Zhang, C. L. Shao, X. H. Li, L. Zhang, H. M. Xue, C. H. Wang, and Y. C. Liu, J. Phys. Chem. C. 114 (2010) 7920.
[18] Jun Zhang, R. Skomski, L.P. Yue, Y.F. Lu, D.J. Sellmyer, J. Phys. Condens. Matter. 19 (2007) 256204.
[19] C.B. Fitzgerald, M. Venkatesan, L.S. Dorneles, R. Gunning, P. Stamenov, J.M.D. Coey, P.A. Stampe, R.J. Kennedy, E.C. Moreira, U.S. Sias, Phys. Rev. B. 74 (2006) 115307.
[20] N. H. Hong, J. Sakai, W. Prellier and A. Hassini, J. Phys.: Condens. Matter. 17 (2005) 1697.
[21] C.B. Fitzgerald, M. Venkatesan, L. S. Dorneles, R. Gunning, P. Stamenov, J. M. D. Coey, Li. A. Stampe, R. J. Kennedy, E. C. Moreira and U. S. Sias, Phys. Rev. B: Condens. Matter Mater. Phys. 74 (2006) 115307.

[22] J. M. D. Coey, A. P. Douvalis, C. B. Fitzgerald, M. Venkatesan, Appl. Phys. Lett. 84 (2004) 1332.
[23] A. Punnoosea, K.M. Reddu, J. Hays, A. Thurber, M. H. Engelhard, Appl. Phys. Lett. 89 (2006) 112509.
[24] S.K. Misra, S.I. Andronenko, K.M. Reddy, J. Hays, A. Punnoose, J. Appl. Phys. 99 (2006) 08M106.
[25] Nguyen Hoa Hong, Joe Sakai, Ngo Thu Huong, Nathalie Poirot, Antoine Ruyter, Phys. Rev. B. 72 (2005) 045336.
[26] S.J. Ding, D.Y. Luan, F.Y.C. Boey, J.S. Chen and X.W. Lou, Chem. Commun. 47 (2011) 7155.
[27] W. Zhou, R. Liu, Q. Wan, Q. Zhang, A. Pan, L. Guo, and B. Zou, J. Phys. Chem. C. 113 (2009) 1719.
[28] C. Wang, Q. Wu, H. L. Ge, T. Shang, and J. Z. Jiang, Nanotechnology. 23 (2012) 075704.
[29] G. Rahman, V. M. Garcıa-Suarez, J.M. Morbec, J. Magn. Magn. Mater. 328 (2013) 104-108.
[30]H. X. Luan, C. W. Zhang, F. Li, P. Li, M. J. Ren, M. Yuan, W. X. Ji, P. J. Wang, RSC Advances. 4 (2014) 9602.
[31] B. J. Huang, F. Li, C. W. Zhang, P. Li, P. J. Wang, J. Phys. Soc. Jpn. 83 (2014) 064701.
[32] G. Kresse, J. Hafner, Phys. Rev. B. 47 (1993) 558.
[33] K. Schwarz, P. Blaha, G. Madsen, Comp. Phys. Commun. 147 (2002) 71-76.
[34] J. P. Perdew, K. Burke, M. Ernzerhof, Phys. Rev. Lett. 77 (1996) 3865.
[35] V. I. Anisimov, F. Aryasetiawan, and A.I. Lichtenstein, J. Phys.: Condens. Matter 9 (1997) 767.
[36] H. J. Monkhorst, J. D. Pack, Phys. Rev. B. 13 (1976) 5188.
[37] Mak KF, Lee C, Hone J, Shan J, Heinz TF. Phys. Rev Lett . 105 (2010) 136805
[38]T. He, M. W. Zhao, X. J. Zhang, H. Y. Zhang, Z. H. Wang, Z. X. Xi, X. D. Liu, S. S. Yan, Y. Y. Xia, and L. M. Mei,J. Phys. Chem. C. 113 (2009) 13610.
[39] J. M. Themlin, R. Sporken, J. Darville, R. Caudano, J. M. Gilles, R. L. Johnson, Phys. Rev. B. 42 (1990) 11914.
[40] M. A. Maki-Jaskari, T. T. Rantala, Phys. Rev. B. 64 (2001) 075407.
[41] A.F. Kohan, G. Ceder, D. Morgan, Chris G. Van de Walle, Phys. Rev. B. 61 (2000) 15019.
[42] Errico L A, Renterıa M and Weissmann M, Phys. Rev.B. 72 (2005) 184425.
[43] P. Guss, M.E. Foster, B.M. Wong, F.P. Doty, K. Shah, M.R. Squillante. U. Shirwadkar, R. Hawrami, J. Tower, and D. Yuan. J. Appl. Phys. 115 (2014) 034908.
[44] F. Wooten, Optical properties of solids (Academic, New York, 1972). Chap, 2, 152.
[45] M. Naeem, S. K. Hasanain, A. Mumtaz, J. Phys : Condens. Matter. 20 (2008) 025210.

Table I: The bond length between the sit of *X* atom and its nearest O atoms($d_{x\text{-}o}$), the defect formation energy (E_f) whose plus and minus represent the absorbing and releasing energy, the total magnetic moment (M) , the total magnetic moment with GGA+U method (M_u) and the local magnetic moment for TM atom (M_x) whose plus and minus represent spin-up an spin-down, the charge transfer for TM atom (Q) whose minus represent losing electron.

Configurations	$d_{x\text{-}o}$	E_f	M	M_u	M_x	Q
SnO_2	2.11	--	0	--	--	--
Cr:SnO_2	1.97	-0.56	2	2	1.97	-1.80
Mn:SnO_2	1.96	-0.37	-3	-3	-2.85	-1.73
Fe:SnO_2	1.95	+0.35	2	2	1.91	-1.57
Ni:SnO_2	1.95	+1.75	0	0	0	-1.34

Figure 1 (a) Top view of pure SnO_2NSs (the position of Sn is denoted by X) (b) side view of pure SnO_2NSs (c)TDOS of pure SnO_2NSs (d) the band structure of pure SnO_2NSs

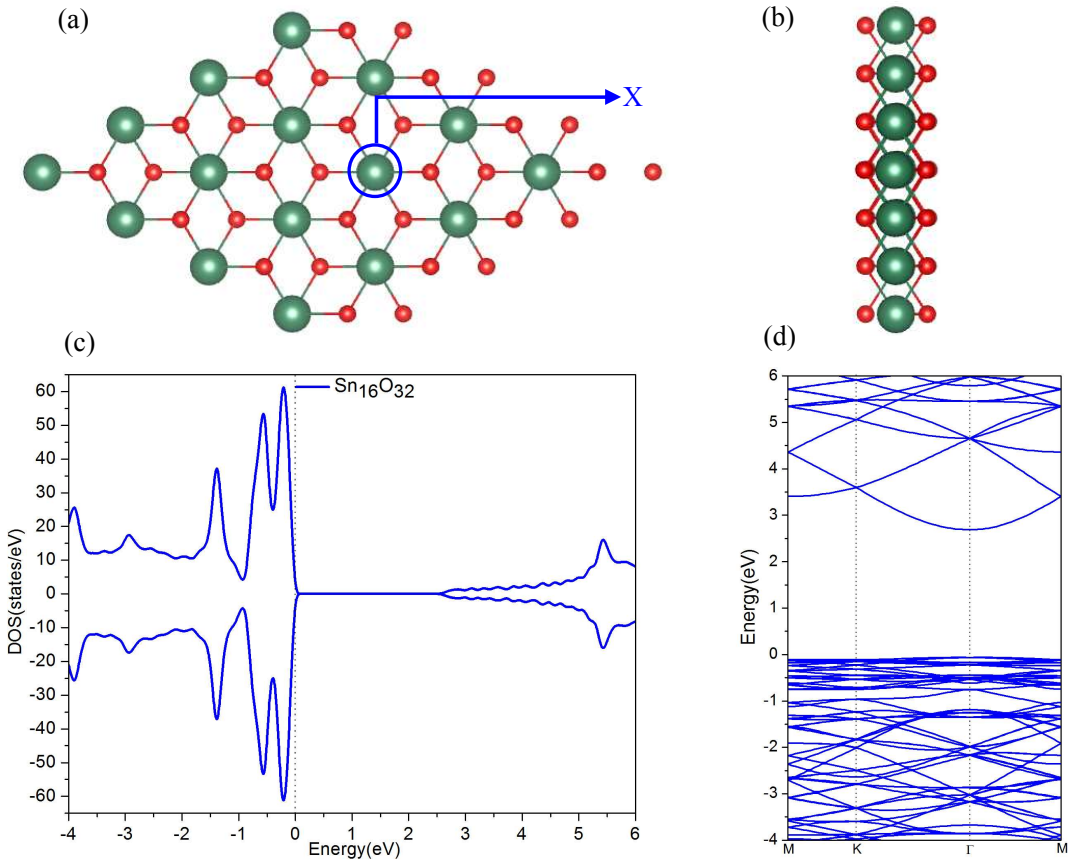

Figure 2 Total and partial DOS for (a) Cr, (b) Mn, (c) Fe, and (d) Ni adatom and nearest O, Sn atoms. Fermi level is set to zero. DOS is broadened by Gaussian smearing with 0.2 eV.

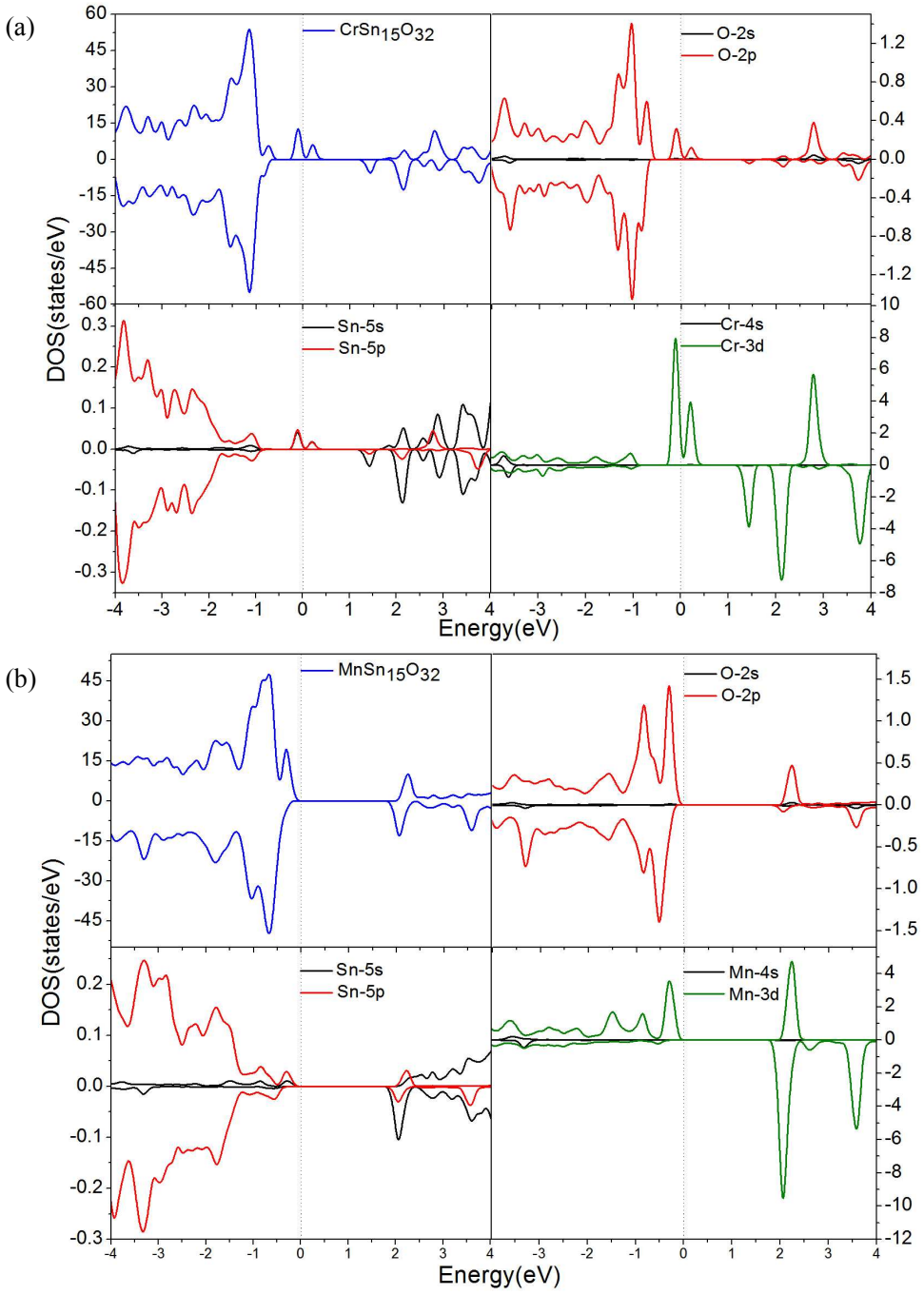

(c)

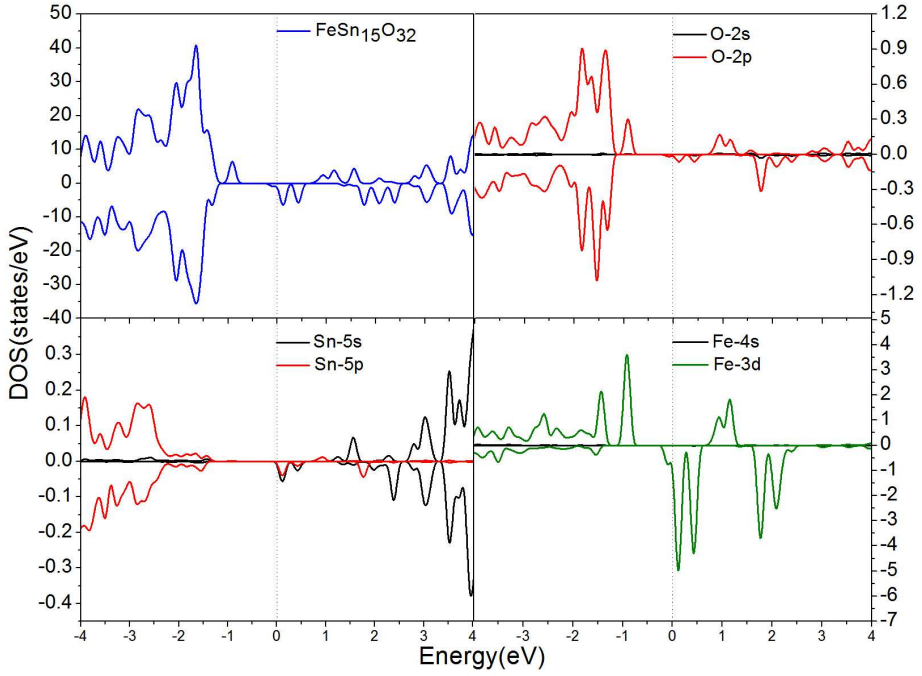

(d)

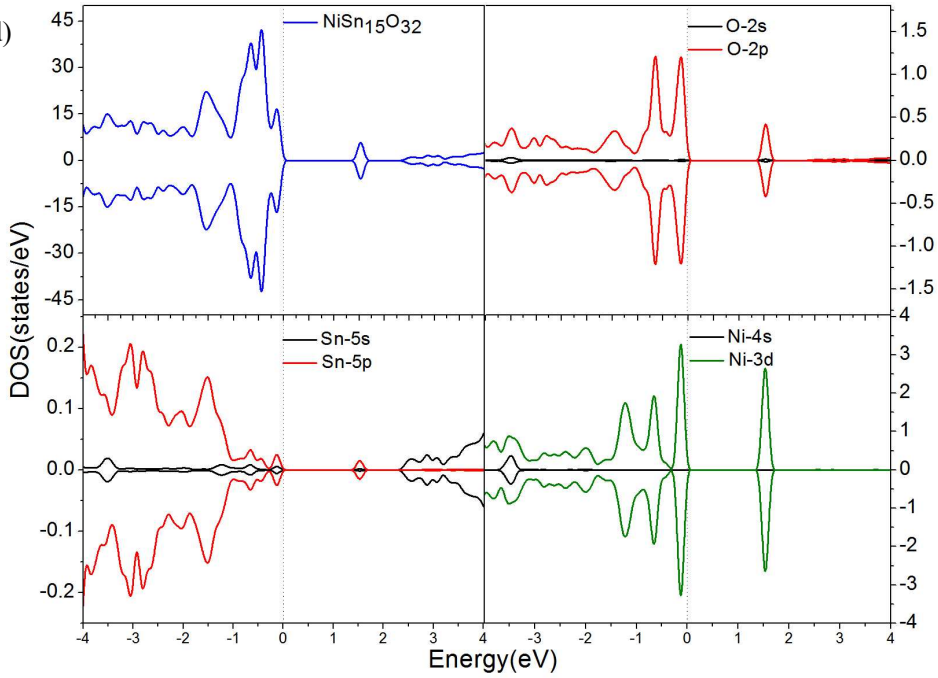

Figure 3 The spin density distribution of TM-doped SnO_2NSs. (a) Cr-doped SnO_2NSs (b) Mn-doped SnO_2NSs (c) Fe-doped SnO_2NSs (d) Ni-doped SnO_2NSs, yellow and blue represent spin-up and spin-down.

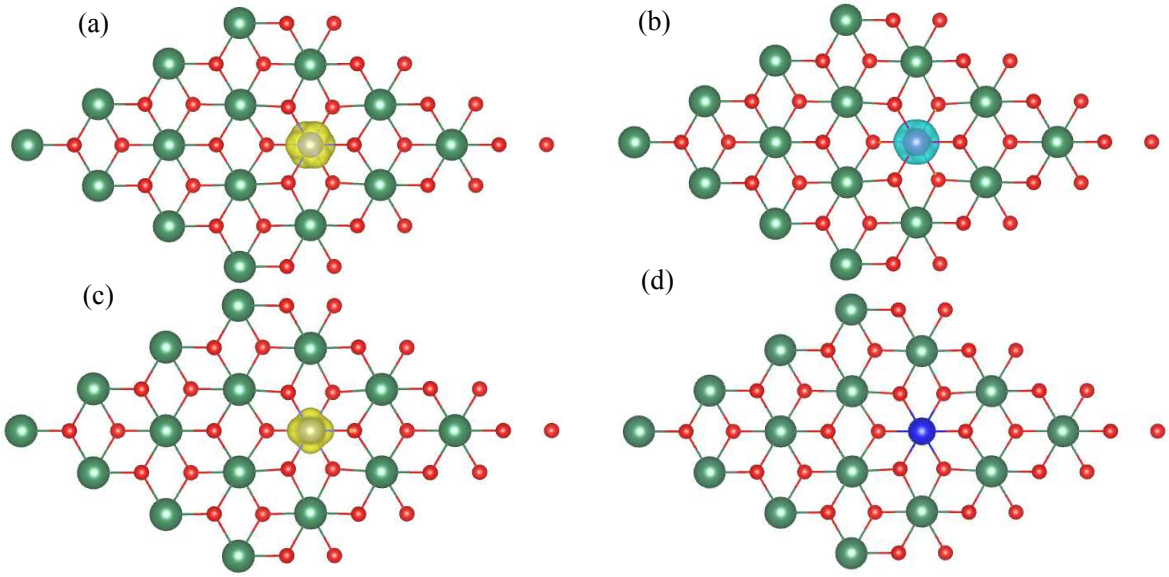

Figure 4 Electronic band structures for (a) Cr, (b) Mn, (c) Fe and (d) Ni adsorbed stanene. Fermi level is set to zero. The arrows ↑ and ↓ represent spin-up and spin-down, respectively.

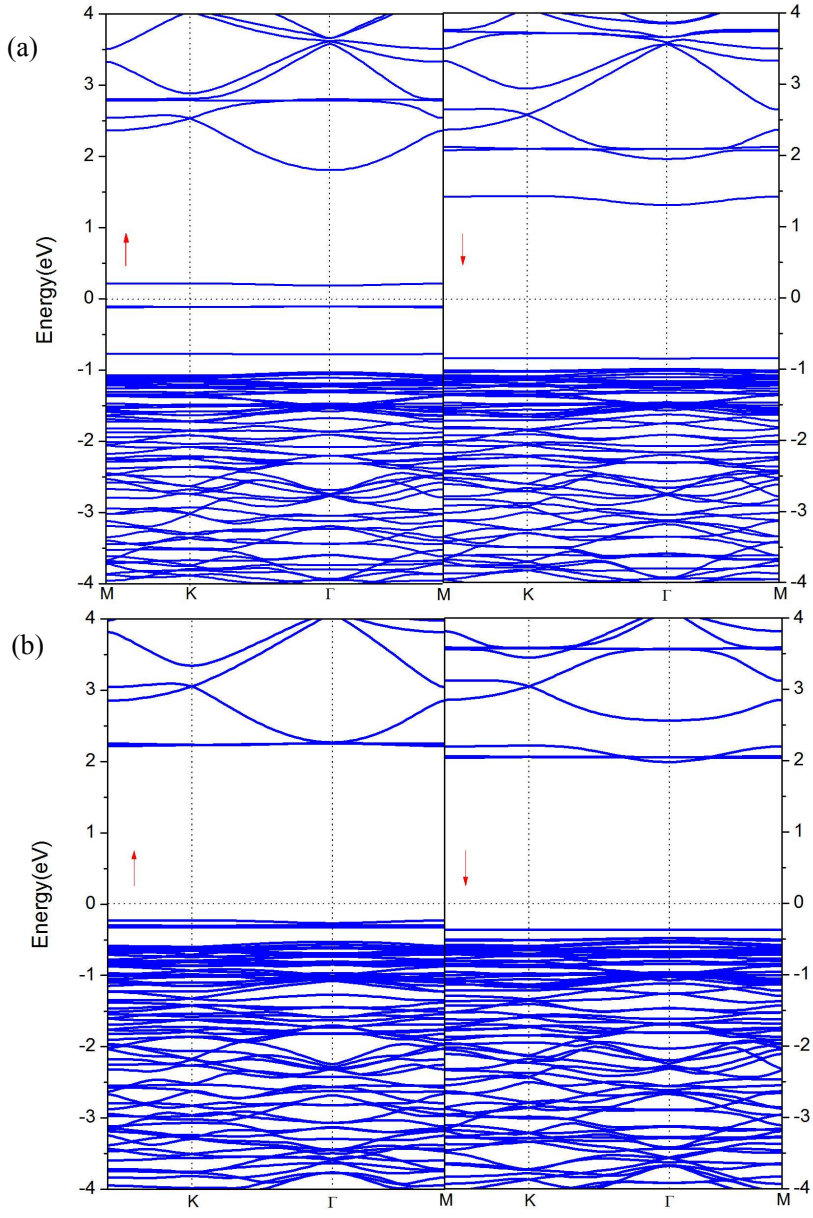

(c)

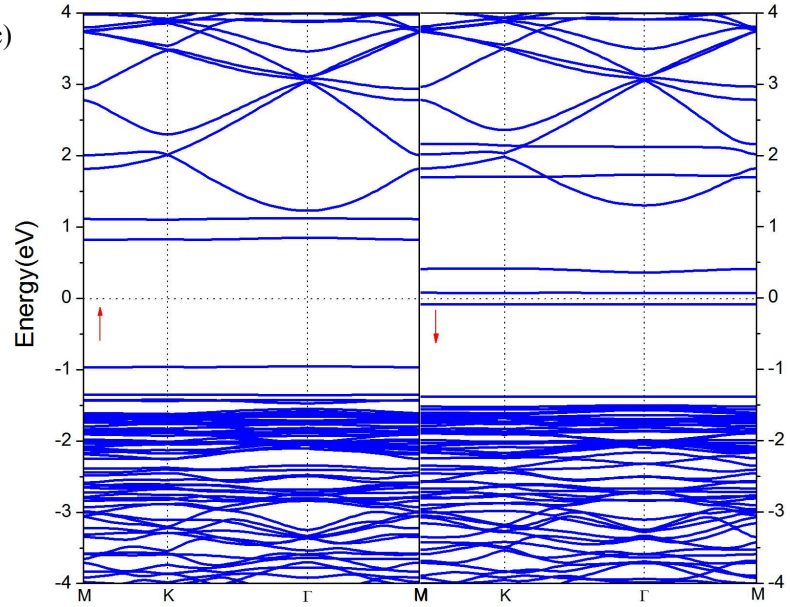

(d)

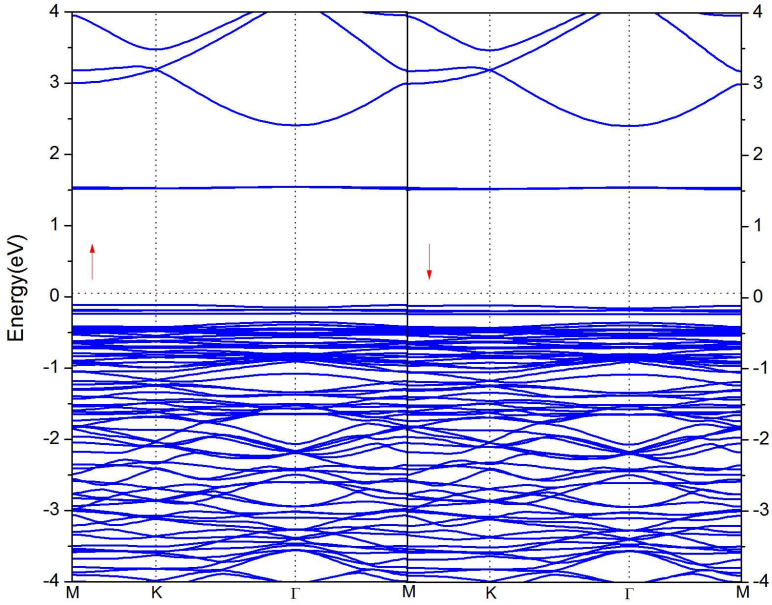

Figure 5 Total and TM atom 3*d* partial DOS with U=3 (a) Cr, (b) Mn, (c) Fe, and (d) Ni. Fermi level is set to zero. DOS is broadened by Gaussian smearing with 0.2 eV.

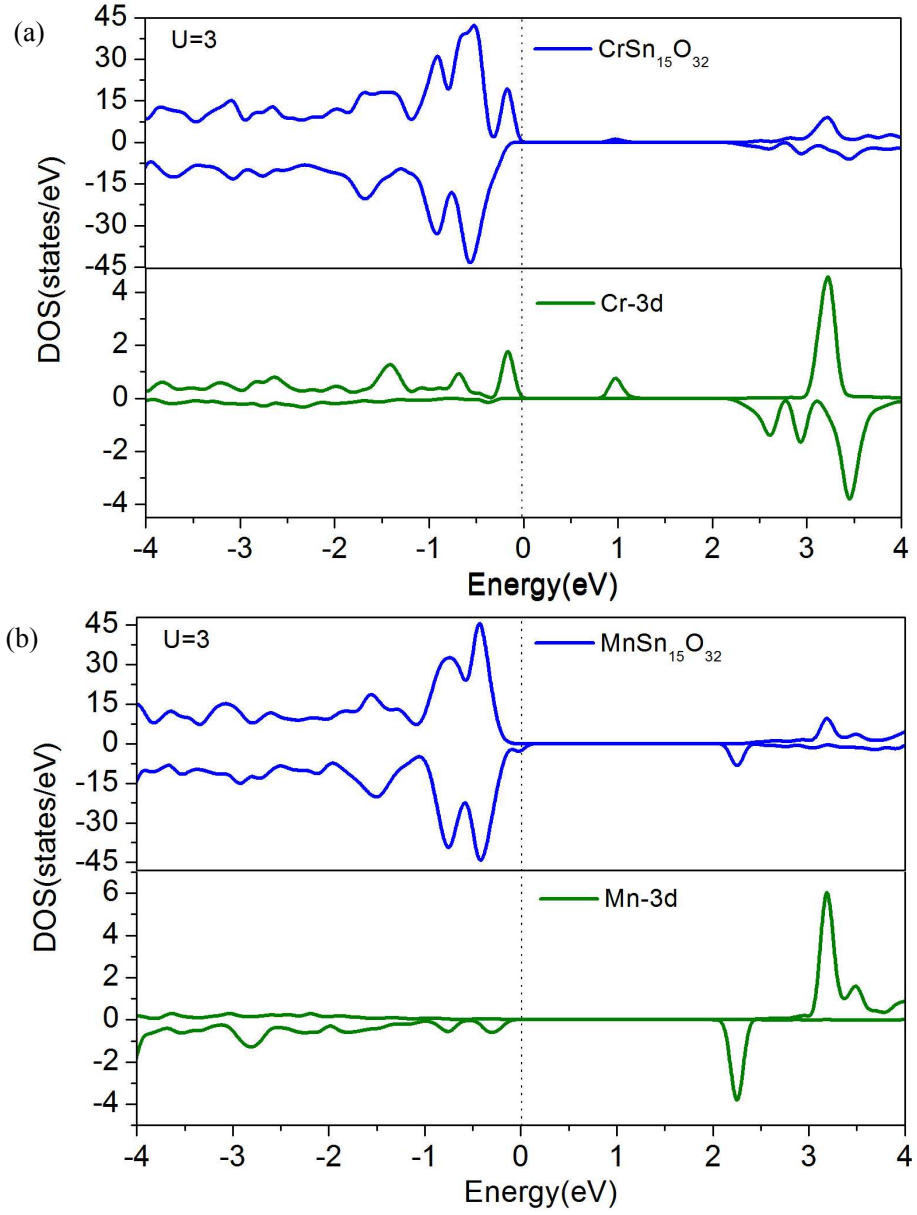

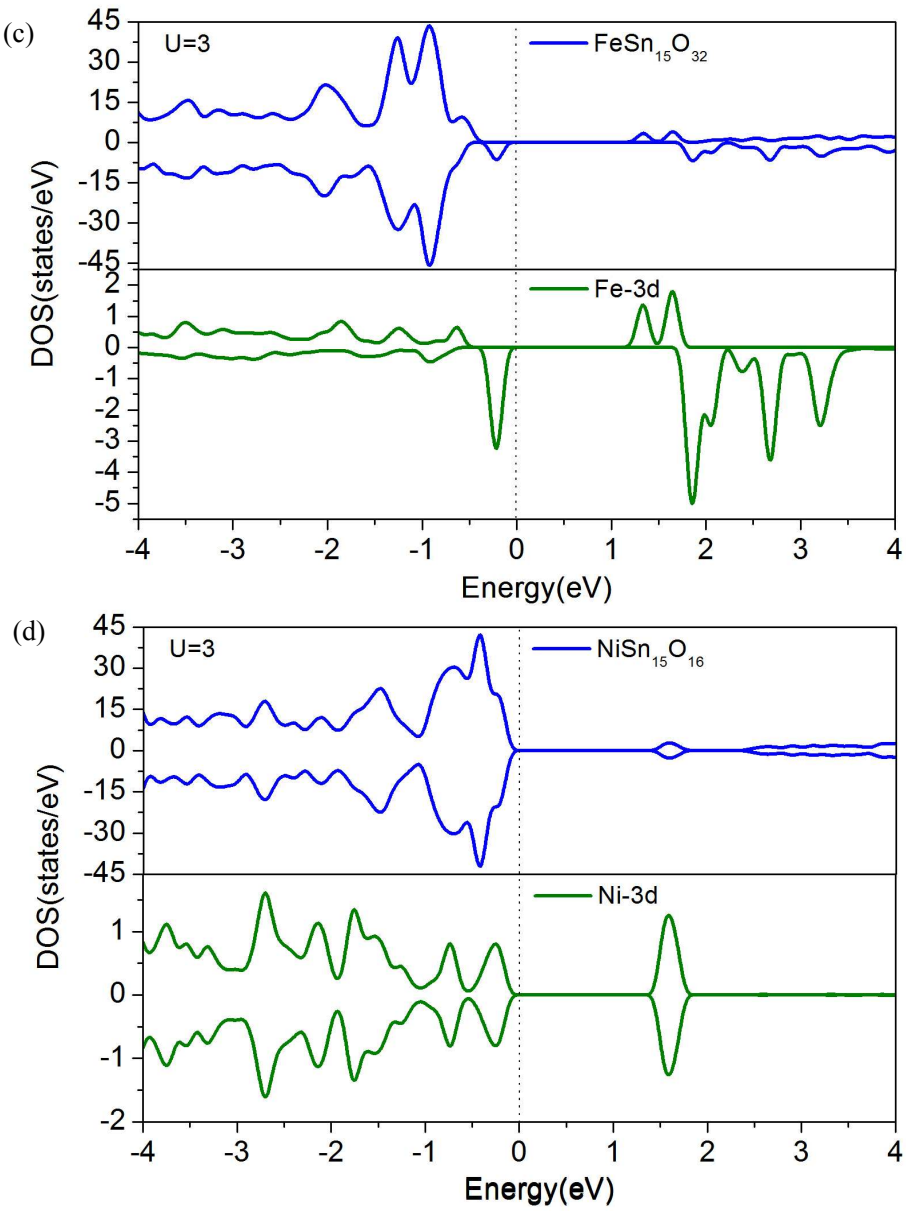

Figure 6 (a) The dielectric functions of pure SnO_2NSs and TM atom doped SnO_2NSs (b) Optical absorption coefficient of pure SnO_2NSs and TM atom doped SnO_2NSs

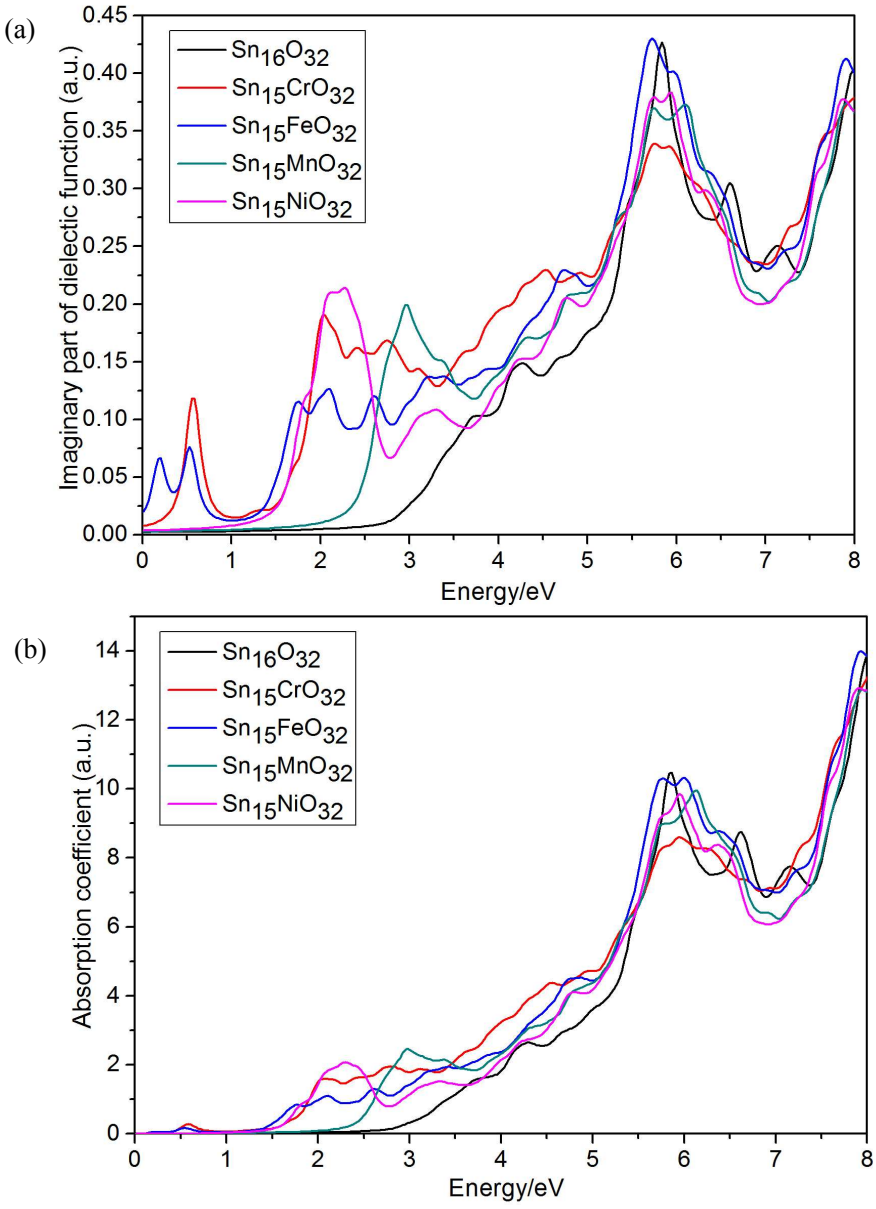

Figure 7 (a) The reflectivity of pure SnO_2NSs and TM atom doped SnO_2NSs (b) refractivity of pure SnO_2NSs and TM atom doped SnO_2NSs